BENCH METHODS FOR BEAM-COUPLING IMPEDANCE MEASUREMENT

F. Caspers
CERN, Geneva, Switzerland

1. INTRODUCTION

The coaxial-wire method is a wide-spread tool for bench measurements of beam-coupling impedance. By introducing a wire into the vacuum chamber under test, a surface current distribution on the inner surface of the beam pipe will be obtained which corresponds approximately to the current distribution produced by a passing particle bunch. When this image-current distribution has been perturbed by a discontinuity (e.g. change in pipe diameter) a reaction on the wire takes place similar to the reaction of a wake field on the particle bunch. Since the wire, which should be located on the axis of the particle beam, transforms the empty beam pipe into a coaxial line, a new boundary value problem is created and one has to be aware of the limits of validity of this simulation method. The maximum characteristic impedance of such a coaxial line can be, at best, several hundred ohms. This has to be compared with the impedance of the beam, which is infinite, and thus represents a current source. Furthermore, the phase velocity of the line must approximate to the beam velocity. Therefore, the simulation is rather easy for a highly relativistic beam ($\beta = v/c \approx 1$) but may lead to some difficulties for small β (at least in the case of longitudinal impedance measurements).

For longitudinal impedance and loss-factor measurements, the set-up consists of a single wire (thin, in order to approximate $Z_L = \infty$) in the center of the vacuum chamber (at the position of the beam). For transverse measurements one may use either two parallel wires (dipole excitation, high common-mode rejection required) or an image plane (metal plate), with a single wire on one side. Both methods have been applied for pick-up and kicker measurements. Both have advantages and disadvantages and the decision for one or the other depends on the particular problem. For the

field simulation of slow beams where the ratio of E/H is not equal to 377Ω, a technique using individually excited probes and loops is described. Since it is tedious to install the coaxial wire in certain cases, measurements on waveguide modes may be carried out. For reflection this is analogous to the well-known time-domain reflectometry, except that the lowest frequency is given by the cut-off wavelength of the beam pipe. In transmission using TM_{on} modes valuable information on the beam-coupling impedance can be revealed.

In this paper, mainly a discussion of practical aspects of several measurement methods will be given, including limits of validity, pitfalls, and a number of examples. Since the coaxial-wire method is in general not very well suited to high impedance and/or high-Q cavity-like objects, the bead-pull perturbation measurement technique to determine R/Q is also briefly discussed.

2. *WAKE POTENTIALS AND IMPEDANCE*

The electromagnetic field of a point charge moving in free space with constant velocity $\vec{v}$ is given as [1,2]

$$\vec{E} = \frac{q\,\vec{r}_0}{4\pi\,\varepsilon_0\,r_0^3}\,\frac{1 - v^2/c^2}{(1 - (v^2/c^2)\sin^2\psi)^{3/2}} \tag{2.1}$$

$$\vec{B} = \frac{1}{c^2}\,\vec{v} \times \vec{E} \tag{2.2}$$

where $\vec{r}_0$ = vector from the charge to the test particle position,

ψ = angle between $\vec{r}_0$ and $\vec{v}$.

For the case $v \to c$ this field appears like an infinitely thin disk, to an observer in the laboratory. The ratio E/H in this field disk approaches 377 Ω. If the charge is travelling inside a smooth and perfectly conducting beam pipe the shape of the field is not changed. Only its diameter is limited by the dimensions of the beam pipe. It can be shown that the same field structure is present in a lossless coaxial line with an infinitely thin inner conductor and a δ-pulse propagating in the same direction [1] (Green's function).

The longitudinal wake function $w_\parallel$ for a point charge is defined as the energy loss ΔU of a test particle (q_2) following a point-like bunch (q_1) at a distance s [3-5].

$$\Delta U = q_1 q_2 \cdot w_\parallel(s) \tag{2.3}$$

$$w_\parallel(s,r) = -\frac{1}{q_1} \int_{-\infty}^{+\infty} v \cdot E_z(z,r,t)dt\Big|_{z=vt-s} \tag{2.4}$$

where $E(z,r,t)$ is the electric field of the point-like bunch q_1. The longitudinal impedance $Z_\parallel(\omega,r)$ is defined as the Fourier transform of the point wake function (time dependence $e^{+j\omega t}$),

$$Z_\parallel(\omega,r) = \frac{1}{v} \int_{-\infty}^{+\infty} w_\parallel(s,r)ds\ e^{-j\omega s/v}. \tag{2.5}$$

Very often, one is just considering the case $\vec{v} = \vec{j}_z v_z$ at $r = 0$ (small transverse dimensions of the bunch, v_z only). Then the longitudinal loss factor $k_\parallel$ may be written approximately as

$$k_\parallel = \frac{1}{2\pi} \int_{-\infty}^{+\infty} Z_\parallel(\omega,0) \cdot \left|\frac{\dot{\varrho}(\omega)}{\varrho(0)}\right|^2 d\omega \tag{2.6}$$

with $\dot{\varrho}(\omega)$ being the Fourier transform of a real bunch charge distribution $\varrho(z)$. In what follows the indices of $Z_\parallel(\omega,r)$ are omitted for simplicity.

3. MEASUREMENT SYSTEMS

The shape of the wake field of a charged-particle bunch can be seen from the computation results of Weiland [6] in Fig. 1. Considering the electric field lines as being linked to free charges (beam) and surface currents (beam pipe), one gets some qualitative insight into the interactions of the wake field. Due to a discontinuity, a certain amount of electromagnetic energy is extracted from the bunch and deposited into the near vicinity of, say, the step, or into a cavity. The associated electromagnetic field reacts back on the tail of the particle bunch (causality) and, for cavity-like objects, also on later bunches which are sufficiently close. Since for frequencies below the cut-off frequency (for waveguide modes) of the beam pipe the deposited field energy cannot travel away, it will finally be absorbed due to metallic losses.

a)

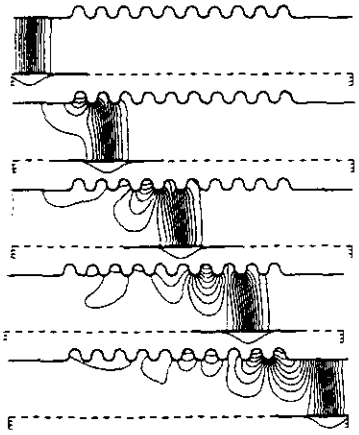

b)

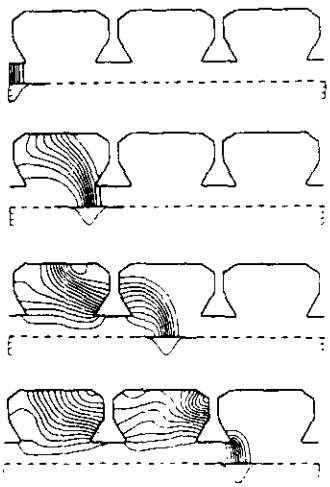

Fig. 1

Electromagnetic field of Gaussian (σ = 1 cm) bunch of charged particles traversing a bellows at the speed of light (side tube radius 6 cm, maximum radius of the bellows section 7 cm). The charge density on-axis is plotted below the symmetry axis [6].

Electric field of a Gaussian bunch (σ = 2cm) traversing 3 cells of a PETRA cavity at the speed of light. Displayed lines (rH_φ = const) show the direction of the electric field and their density is proportional to $\vec{r} \cdot |E|$. The bunch charge density on-axis is plotted below the symmetry axis [6].

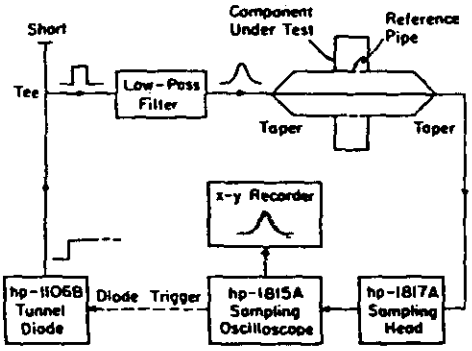

Fig. 2 - *Instrumentation for measuring parasitic mode loss* [7].

A measurement system which is capable of producing a field configuration very closely related to the situation shown in Fig. 1 a) and b) is presented in Fig. 2 [8].

The basic measurement method has been described by Sands and Rees [7]. A fast step with about 20 ps rise time (tunnel-diode generator) passes a

pulse-forming network (shorted tee and low-pass filter). The purpose of the low-pass filter is to adjust the pulse length to the given bunch length. Thus a nearly Gaussian pulse is generated. It travels either through a reference pipe consisting of a straight section of vacuum chamber and a thin wire on the axis of the beam, or the component under test which preferably has the same mechanical length. Both signals, $I_0(t)$ = reference signal = unperturbed case = solid line in Fig. 3, and $I_1(t)$ = object signal = dashed line in Fig.3, are recorded sequentially and stored. Note that a pulse generated this way may have a rather low amplitude (50 to 100 mV). If higher amplitudes are required, pulse generators with an avalanche transistor and sometimes an additional step recovery diode have been used.

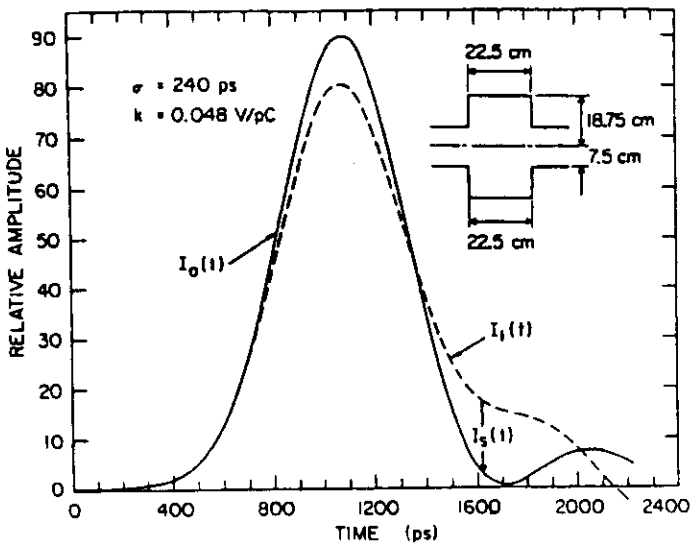

Fig. 3 - Recorded output pulses ($I_0(t)$ for the reference pipe and $I_1(t)$ for a cylindrical cavity having the dimensions shown [8].

For evaluation of the loss factor k (having dimensions volt/coulomb) the following relations hold:

$$k(\sigma) = \frac{2Z_0}{Q^2} \int I_0(t) I_S(t) dt \qquad (3.1)$$

with $Q = \int I_0(t) dt$ = charge in the pulse,

$I_S(t) = I_0(t) - I_1(t)$ = subtracted signal,

Z_0 = characteristic impedance of the coaxial line formed by the vacuum chamber with the wire,

σ = rms length of the Gaussian pulse (bunch length $\approx 4\sigma$).

In practice the limits of the integral in Eq. (3.1) extend from $\tau-2\sigma$ to $\tau+2\sigma$ with τ = position of the maximum of $I_0(t)$. This truncation already implies a time-filtering process omitting wake-field effects coming later than $\tau+2\sigma$. Since the loss factor is related only to the real part of the coupling impedance [8] by

$$k = \sum_n (\omega_n/4)(R/Q_n) \exp(-\omega_n^2\sigma^2), \tag{3.2}$$

the influence of the imaginary part, which would contribute to a delay between $I_0(t)$ and $I_1(t)$ has to be removed by superimposing both pulses in the knee region (i.e. 400 ps to 600 ps, Fig. 3) using some adequate correlation technique. It turns out that for properly positioned $I_1(t)$ the loss factor k is not sensitive to small shifts between $I_0(t)$ and $I_1(t)$. $I_0(t)$ and $I_1(t)$ may be recorded simultaneously with a modified measurement system (two sampling heads). In this case drifts of the timing system in the sampling scope do not need to be removed by the correlation procedure.

It should be pointed out that by omitting the influence of the imaginary part of the beam-coupling impedance, valuable information may be lost. In certain cases (e.g. bellows) the imaginary part at lower frequencies is of interest (for determination of Z/n). Using this method it can be deduced from the real part measured around some resonances at higher frequencies and applying Hilbert transforms.

A rather similar measurement system to that depicted in Fig. 2 (operated in the time domain) is shown in Fig. 4 for frequency domain measurements [9] which are straightforward. The output signal of an rf generator of variable frequency is split symmetrically. One part passes the reference line, the other part the measuring line or device under test. The configuration depicted in Fig. 4 may be considered as a primitive network analyzer. Here as well (compared to loss-factor measurements) the difference between reference and object is used to evaluate (approximately) the unknown impedance $Z(\omega)$ (only valid if $Z \ll R_0$). In fact, for simultaneous recording of $I_0(t)$ and $I_1(t)$ the type of measurement bridge shown in Fig. 2 was used at Cornell University in the early eighties [10]. In this case, the correla-

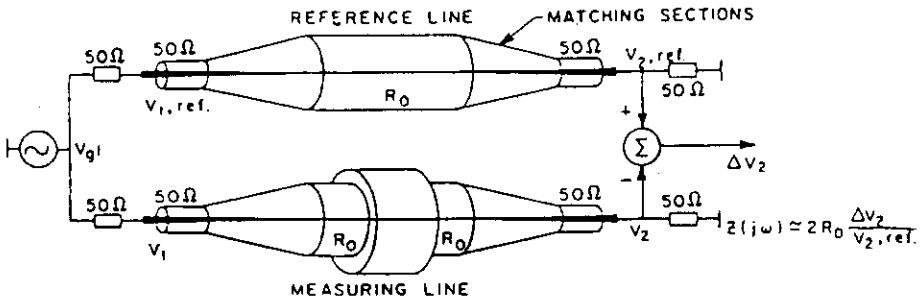

Fig. 4 - Beam-coupling impedance measurement system (frequency domain) [9].

tion method mentioned above has not always been applied and the signal delay was used to evaluate the imaginary part of the beam coupling impedance. High mechanical stability (to 0.1 mm) is required to obtain meaningful results. For a discussion of limitations and possible sources of errors, a brief description of the measurement procedure will now be given.

4. S-PARAMETERS AND IMPEDANCE

Consider a single localized impedance Z (Fig. 5) in a coaxial line (characteristic impedance Z_L)[9]. The S-matrix (S = scattering) of this 2-port or 4-pole system has in general four complex and frequency-dependent elements, namely S_{11} = input reflection coefficient, S_{12} = reverse transmission, S_{21} = forward transmission, and S_{22} = output reflection coefficient.

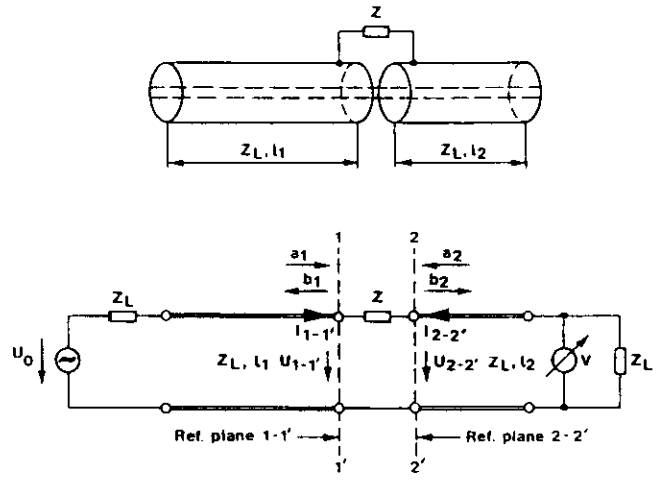

Fig. 5 - S-parameters of a single lumped impedance [11].

The relation between waves travelling towards the 2-port (a_1, a_2) with $|a_1| = (U_0/2)(1/\sqrt{Z_L})$ and those travelling away (b_1, b_2) is given by:

$$\begin{pmatrix} b_1 \\ b_2 \end{pmatrix} = \begin{pmatrix} S_{11} & S_{12} \\ S_{21} & S_{22} \end{pmatrix} \begin{pmatrix} a_1 \\ a_2 \end{pmatrix} \quad \text{or (b)} = S \quad \text{(a)}.$$

For determination of $S_{11} = S_{22}$ and $S_{21} = S_{12}$ the well-known formula for the reflection coefficient ϱ (here $\varrho = S_{11}$) applies and yields

$$S_{11} = \frac{(Z + Z_L) - Z_L}{(Z + Z_L) + Z_L} = \frac{Z}{2Z_L + Z} \quad ; \quad Z = \frac{S_{11} \cdot 2Z_L}{1 - S_{11}} \tag{4.1}$$

$$S_{21} = U_{2-2'}/(U_0/2) = 2Z/(2Z_L + Z_L).$$

Thus the unknown Z can be determined from the measured S_{21} as

$$Z = \frac{2Z_L(1 - S_{21})}{S_{21}} \tag{4.2}$$

or approximately $Z \approx 2Z_L(1 - S_{21})$ for $|Z| \ll Z_L$(cf. Fig. 4).

It should be noted that for a convenient mathematical treatment of cascaded elements the T-matrix (Transfer matrix [12]) instead of the S-matrix may be used:

$$\begin{pmatrix} b_1 \\ a_1 \end{pmatrix} = \begin{pmatrix} T_{11} & T_{12} \\ T_{21} & T_{22} \end{pmatrix} \begin{pmatrix} a_2 \\ b_2 \end{pmatrix}. \tag{4.3}$$

It appears from Eq. (4.2) that it might be rather convenient to determine Z from S_{11} rather than from S_{21} since S_{11} is more sensitive to variations of small Z than S_{21}. But for a proper measurement of S_{11} the precise knowledge of the reference-plane position 1-1' is required. This may be mechanically tedious and sometimes difficult to define. In contrast, for a transmission measurement the location of Z on the line is of no relevance [9]. Furthermore, for a real beam there will be no reflected energy for spectral components below the cut-off frequency of waveguide modes in the beam pipe.

As a somewhat more complicated case a double step in cross section will now be considered [9].

Normally, the electric field energy stored in an abrupt change of diameter of a coaxial line is represented by a parallel capacitor as shown

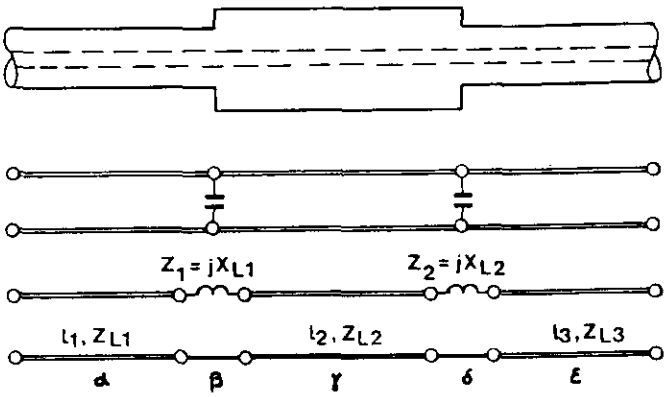

Fig. 6 - Double-step and equivalent circuits [9,11].

in Fig. 6. This equivalent circuit is often used to describe the S-parameters for this type of discontinuity on a coaxial line both in transmission and reflection. The parallel element has to be converted into a serial one to represent the interaction with a particle beam of infinite impedance [9,13]. Now the serial inductance is only approximately valid for small perturbations (with respect to Z_L) and only in transmission. In a mathematical model for sections α, β, j, δ and ε either the S- or T-matrices may be evaluated. As shown in Ref. [9] the sum of X_{L_1} and X_{L_2} appears rather clearly from a transmission measurement as an additional phase shift for reasonably small changes in diameter, and the measured results agree well with theoretical data. For reflection measurements, errors of a factor 30 have been found. It turns out that, as a general rule [9], the S-parameter for beam coupling impedance is better measured by transmission than by reflection. However, one has to ensure that transmission data are not perturbed by parasitic effects. For the example in Fig. 6 a considerable amount of reflected energy is due to the change in characteris impedance (Z_{L_1};Z_{L_2}) in addition to jX_{L_1} and jX_{L_2}, respectively. Even if generator and load are perfectly matched some scattered energy will travel back and forth between X_{L_1} and X_{L_2} which would not be the case for the empty beam pipe.

For small perturbations one may write

$$|S^{\beta}_{21}| = \sqrt{(1 - |S^{\beta}_{11}|^2)} \approx 1 - \frac{|S^{\beta}_{11}|^2}{2} . \qquad (4.4)$$

For example, $S^{\beta}_{11} = 0.1 \Rightarrow S^{\beta}_{21} = 0.995 \Rightarrow \Delta U = 0.5\%$. Thus there is little change in the voltage of the transmitted wave, but a rather large reflection (voltage of the reflected wave). In the case of two discontinuities (β and δ) and $Z_{L_1} = Z_{L_2}$ one obtains in transmission $\Delta U \approx 1\%$. But the reflected wave ($b_{1\delta}$) from jX_{L_2} travels back to jX_{L_1}, is reflected again ($b_{2\beta}$) (now going forward), and appears superimposed on the transmitted wave after $jX_{L_2}(b_{2\delta})$. Taking the numbers from above with $b_{1\delta} = 0.1$ and $a_{2\beta} = 0.01 = 1\%$ the measurement error of $\Delta U = 1\%$ is just equal to twice the change in amplitude relevant for the beam-coupling impedance. This implies that measurement errors can be easily induced by multiple reflections.

In the measurement system of Fig. 4 with distributed transformers on both ends of the beam pipe, one must keep in mind that at lower frequencies the cones look like a step. Often the inner conductor is not tapered in order to maintain a constant impedance over all the length (like an adaptor from an N connector to a 10-cm-diameter coaxial power line). Serious errors due to multiple reflections from the generator or load will then occur for a single discontinuity. Thus the double-step problem in Fig. 6 really becomes a quadruple-step problem. Since normally 50 Ω rf instrumentation is used, some sort of (resistive) broadband matching network to adapt to, say, 150 Ω is required in addition to a tapered center conductor [14]. This type of construction is limited by practical difficulties to about 150 Ω characteristic impedance Z_L. In most cases the highest possible values for Z_L should be chosen. A simple very thin wire may be used, but then one has to work either in the time domain (loss factor) with implicit time filtering (Fig. 2) or, if frequency domain results (impedance) are required, the frequency domain data can be used only after time filtering [14].

It should be mentioned that the rule of taking the highest characteristic impedance wherever possible has one exception. That is when the object being measured has such a small impedance that the change in amplitude of the transmitted wave disappears in the measurement noise and uncertainty. In such a case (e.g. short bellows) a large-diameter inner conductor (50 Ω) will give better results than a very small one. Of course, measurements may be carried out using different diameters of the center conductor as a cross check for the validity of results obtained.

With the availability of computer-controlled network analyzers the measurement system of Fig. 4 and Fig. 2 may be improved. The technique shown in Figs. 7 and 8 consists of generating a synthetic pulse in the time domain via FFT from measurements taken in the frequency domain. This leads to higher spectral density than real time or sampling oscilloscope pulse measurements, thus giving a higher dynamic range and better reproducibility. The method (synthetic pulse) has been known since about 1960 [15] but became more readily accessible in 1984 with the introduction of computer-controlled network analyzers. An early version (1983) consisting of separate units from different manufacturers (signal generator, vector analyzer, etc.) was replaced in 1984 by a single network analyzer with a calibration facility and was capable of storing and comparing sequential object and reference measurements (Fig. 7). The corresponding flow diagram (Fig. 8) explains the measurement procedure. In contrast to Fig. 4, the complex quotient of

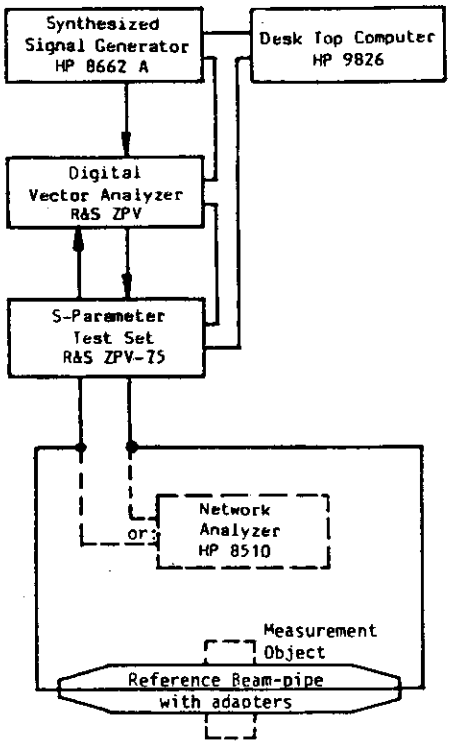

Fig. 7 - Computer-controlled network analyzer system for frequency and time domain measurements [14].

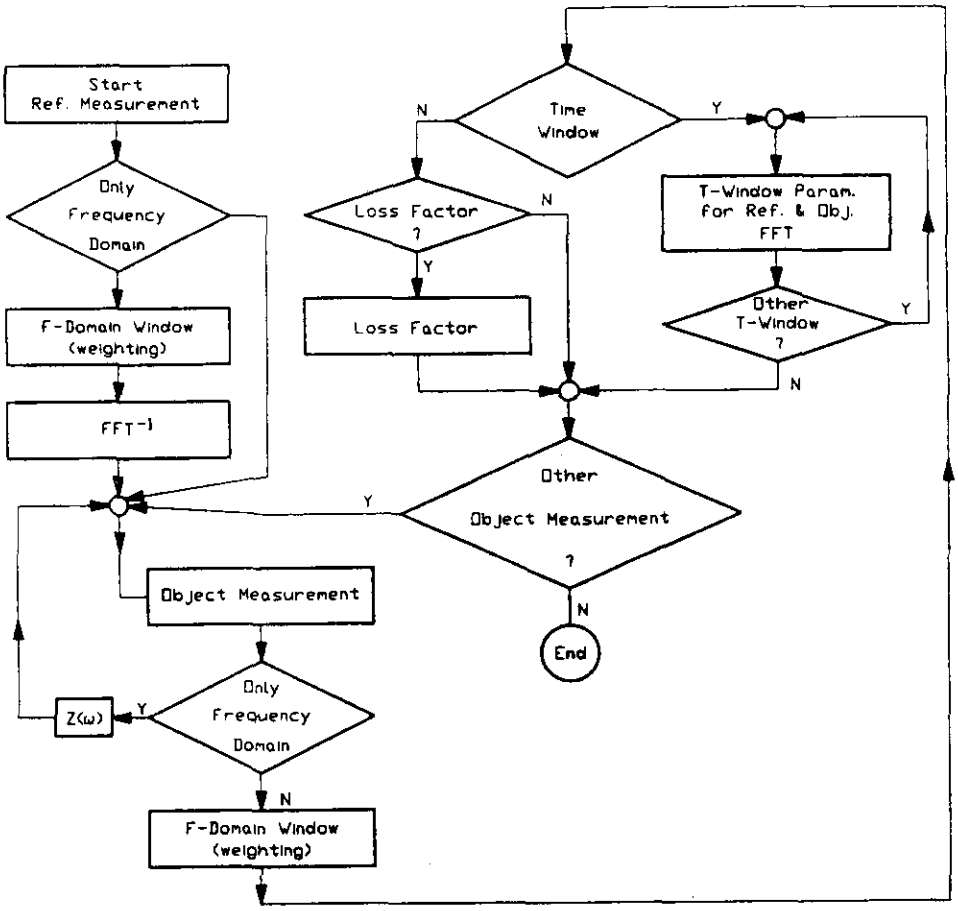

Fig. 8 - Simplified flow diagram for measurement procedure [14].

object and reference measurement can now be evaluated, instead of the difference which gives acceptable results for small impedances only. The possible use of the synthetic pulse method for loss-factor measurements was already mentioned by Sands and Rees in 1974 [7].

As modern network analyzers offer the application of "de-embedding" procedures using different error models, one may remove the influence of badly matched tapers or other transitions with a properly chosen calibration routine [16-26]. De-embedding essentially means that the electromagnetic properties of non-perfect cables, connectors, tapers, etc., are

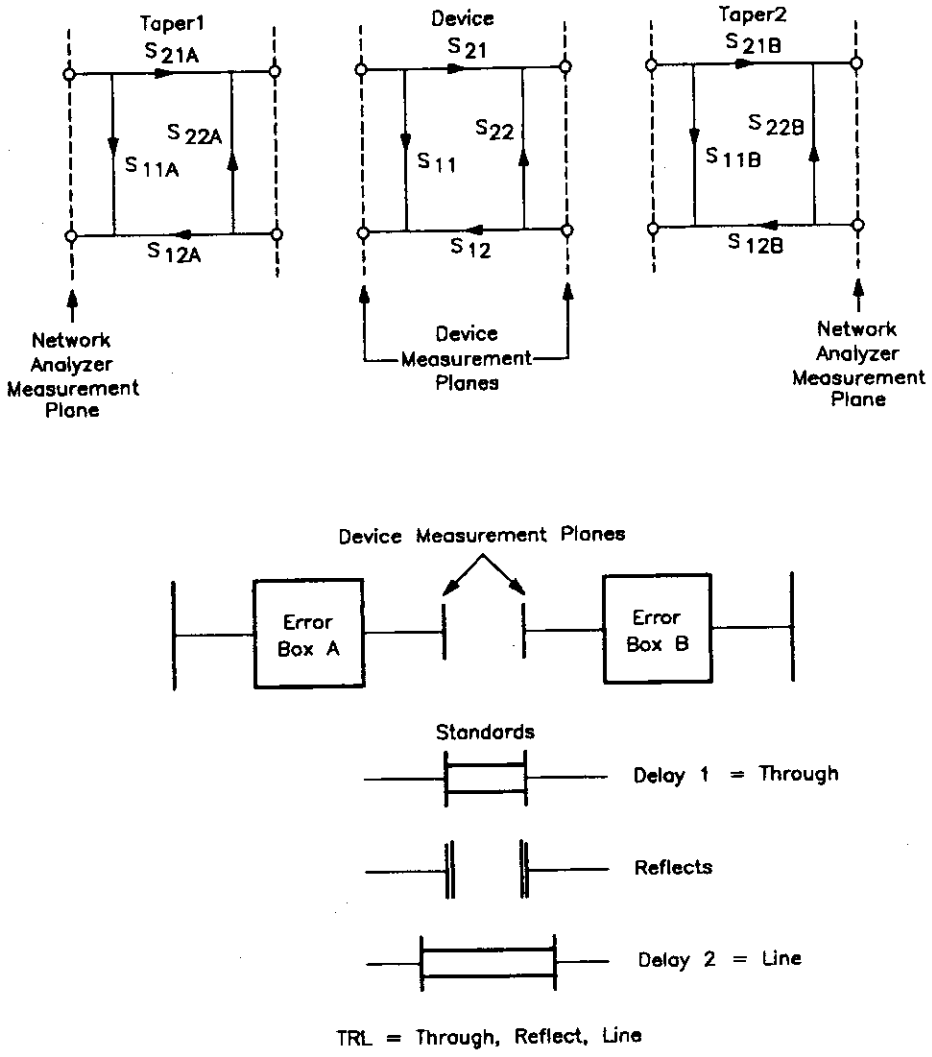

Fig. 9 - A functional block diagram of two-port error-corrected measurement system. TRL-calibration procedure.

determined by measuring several calibration standards (often: open, short, load). With all elements of the T-matrix known, that T-matrix is multiplied with its inverse, resulting in a perfect transmission line (Fig. 9). However, since the de-embedding procedures are not always easy to carry out, gating (= time filtering) of the first pulse arriving in transmission

is the preferred method. Only if considerable overlapping occurs between the first pulse, which may have been lengthened by dispersive elements, and following pulses caused by multiple reflections, can gating not be used any more.

This calibration method is particularly useful for transverse impedance measurements (two parallel wires in opposite phase [17]). Here it turns out that a good broadband match from a 50-Ω, 180° hybrid to some parallel-wire line is not easy to realize. But, as mentioned above for longitudinal impedance, the matching problem always exists for a single wire. The influence of this mismatch may either be removed by time-filtering (implicitly done for loss factors and kick-parameters) or by applying the de-embedding method. Independent of all software (time filter, de-embedding) procedures, the mismatch in the hardware should be made as small as possible. This may be accomplished for frequencies up to 1 GHz by placing small (to avoid inductance) carbon resistors in series with the wire in order to match the high impedance of the beam-pipe wire configuration.

In addition, a few lossy ferrite beads on the wire increase the attenuation easily by 10 to 20 dB. This is to prevent the exchange of electromagnetic energy between discontinuities in the beam pipe, which would not "talk" to each other if the wire were not there. Of course, the additional losses of the ferrite beads have also to be taken into account in the reference measurement. However, the use of such ferrite beads as reasonably matched attenuators is limited to frequencies below cut-off (waveguide modes) of the beam pipe.

For transverse impedance or kick-parameter measurements, basically the same systems as already shown in Fig. 2 or Fig. 7 are applied, except that for the excitation one should use two parallel wires (off-phase) (Fig. 10) or a single wire over a metallic image plane [14,18].

Transverse beam-coupling impedance measurements have been carried out by simply displacing the center conductor in one plane and recording the change of S_{21} as a function of the lateral position. But, due to the presence of a strong signal caused by the longitudinal impedance, the evaluation of the much smaller effect from the transverse impedance on S_{21} is difficult to carry out.

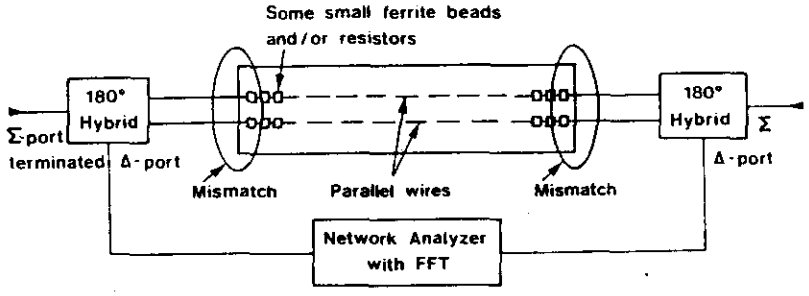

Fig. 10 - Transverse impedance measurement system (2 wires) [11].

A different matter is the transverse response [27] measurement of a pick-up or kicker, where the transmission from the coaxial wire to the pick-up electrodes is considered. Here, it is common practice to displace the wire (provided the coupling impedance is not too high) and to look at the Σ and Δ signal from the pick-up outputs.

Thus, it is important to ensure that for transverse IMPEDANCE measurements a high common mode rejection can be maintained. Broadband (2 MHz to 5 GHz) 180° hybrids show a common-mode suppression of about 30 dB each. With the set-up of Fig. 10 roughly 60 dB common-mode rejection is achievable. The 180° hybrids can easily be included in FFT and also in calibration (de-embedding) routines, in particular those shown in Fig. 9. For the evaluation of Z_T the following approximative relation [18,28] can be used:

$$Z_T = cZ/\omega\Delta^2 \qquad (4.5)$$

where Δ = separation of wires, Z = measured change in transmission line impedance. Note that this relation to evaluate Z_T from a two-wire measurement given in Refs. [28,29] has been derived for the case of a S_{11} measurement with a short-circuit at the far end.

The image plane approach for transverse measurements has the advantage that just one half of the structure to be tested is required. Furthermore, less matching problems occur as a 50-Ω line on a ground plane is easy to realize. Also it is easier to adjust the propagation velocity of the quasi-TEM wave to the β of the beam (usable for $\beta > 0.5$) by means of dielectric material between ground plane and wire. On the other hand, introducing an image plane into a given structure may cause serious difficulties. Therefore it depends on the user which method will be finally chosen. The image

plane method has been extensively used to measure (amongst others) the sensitivity characteristic of CERN-AA (Antiproton Accumulator) pick-ups and kickers (loop PUs). Due to the weak coupling of the fringeing field to the pick-up structure, reliable measurements could be carried out for the transverse response. Here, direct longitudinal measurements with a single wire gave meaningless results, as the longitudinal coupling impedance to be measured was much higher than Z_L. In this case, conclusions on $Z_{\parallel}$ and the longitudinal transfer impedance, derived from the transverse response, were confirmed later from beam observation. The relation between longitudinal and transverse response in pick-ups and kickers have been described in detail by G. Lambertson [30].

5. *REAL-PULSE AND SYNTHETIC-PULSE METHODS*

Comparison of real-pulse and synthetic-pulse measurement techniques shows that the key element, a Schottky diode (or four of them), is just the same. When using a sampling oscilloscope this is the gate of the sampling head, sometimes also referred to as a harmonic mixer, and for the synthetic pulse it is one or more balanced mixers in the rf front end of the network analyzer. The maximum applicable signal for both structures is roughly 1 volt, and due to the duty cycle, an average signal power of the order of microwatts or even less is obtained. From this already low power more than 99% is lost due to the sampling process and the small amount left is spread over a wide frequency range (e.g. 20 GHz). As a consequence, one has to face a rather low spectral density, 1/f noise of the sampling gate, non-linearities, problems with time stability, drifts and jitter. In practice, measurements are carried out over an averaging period of the order of 1 minute, with a usable dynamic range of about 70 dB and a time stability of 1-2 ps. But the measurement process requires careful observation (sudden drifts) and up to 30% of the measured traces have to be rejected because of instabilities during the averageing period [31].

On the other hand, a synthetic-pulse test set-up to 20 GHz or more is much more expensive since a vector network-analyzer, a synthesizer and an S-parameter test set are needed. One has also to ensure that low-frequency spectral components can be measured properly (low f_c of S-parameter test set = directional couplers), otherwise the base line of the time domain

trace might be very unstable. Trying to save money by using a sweep-generator instead of a synthesizer may not pay off as, due to frequency drifts of the sweeper (via calibration), the amplitude and time ($\propto$ phase) stability of the system deteriorates. The dynamic range of a properly assembled synthetic-pulse test set can be 100 dB, with an amplitude stability of 0.01 dB (30 minutes) and a time stability of 1 ps (30 minutes).

6. EXAMPLES OF MEASUREMENTS

As a first case, results for a "bumper" magnet [18] are given in Fig. 11. This example is typical for certain kicker magnet structures whose resonances (obviously) depend on the external loading condition (terminations). One can recognize very clearly the mutual dependence of the real and imaginary part around resonance. Measurements were carried out with a 1.6-mm-diameter wire.

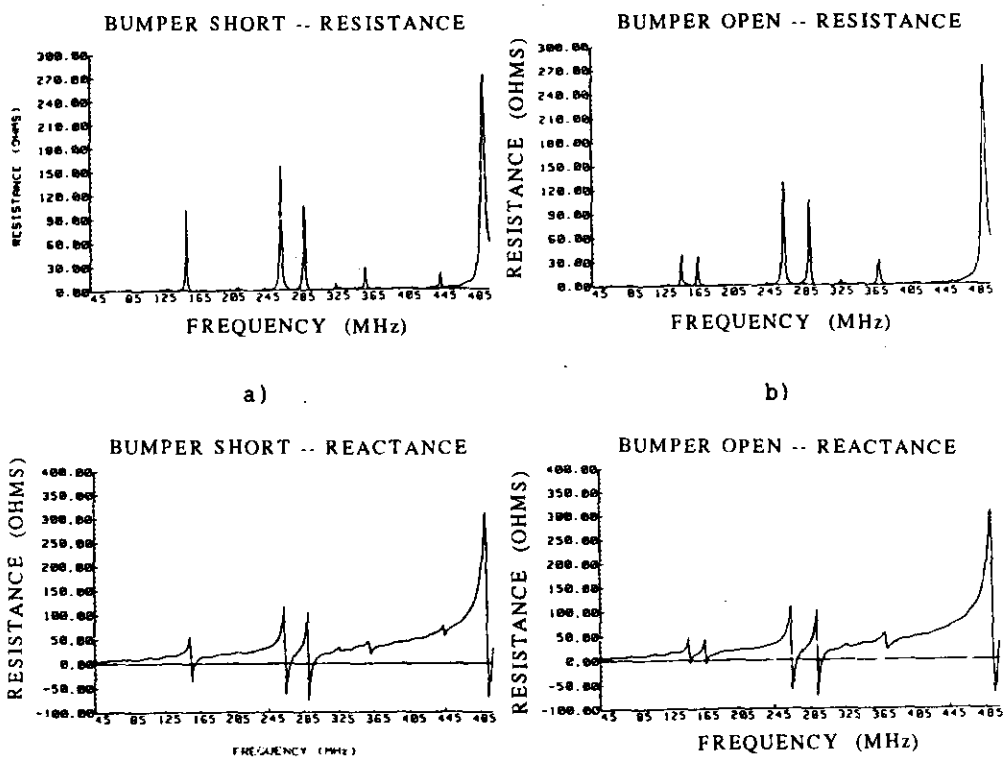

Fig. 11 - Longitudinal impedance of bumper magnet with plates disconnected and magnet electrodes shorted (a) and left open (b) [18].

The results shown in Fig. 12 [18] demonstrate a good agreement between measurement and theory for a device with a single low-Q resonance. A typical bellows (ID 100 mm, OD 120 mm, length 38 mm with six undulations) was measured in transmission and reflection mode using time filtering. The beam coupling impedance (imag. part) resulting from the transmission measurement was checked to be independent (within ±10%) of Z_L (50 Ω < Z_L < 150 Ω) [14]. Good agreement was also found with results obtained by analytical and numerical approaches [32]. The apparent energy loss indicated by the decrease of $|S_{21}|$ (0.02 dB at 1 GHz) is in fact explained by the measured reflected power. In this case, the changes in S_{21} due to the device under test were 1° in phase and 0.02 dB in amplitude. Very good connectors and a stable mechanical and electrical system (semi-rigid cables) are required here.

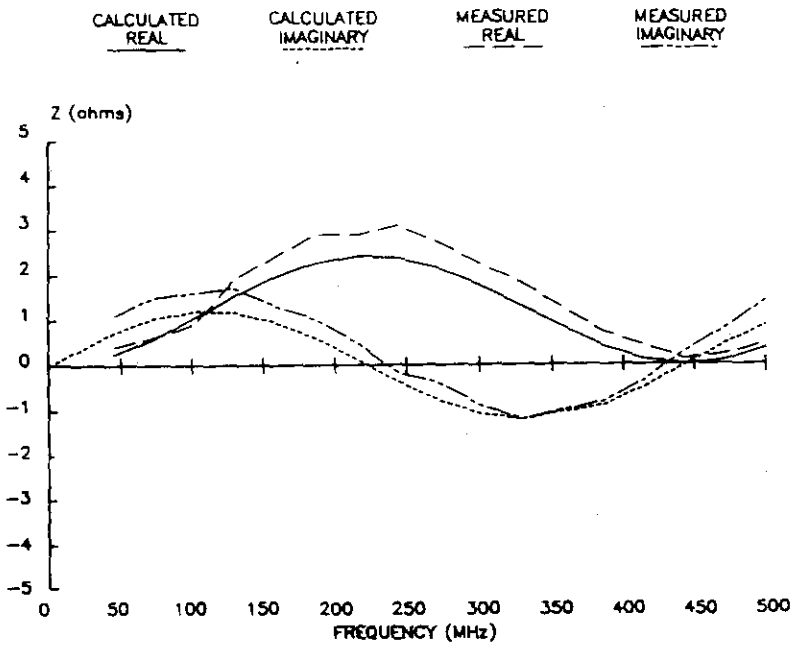

Figure 12 - Longitudinal impedances measured by stripline BPM [17].

A more detailed discussion and other examples are given in Refs. [11,18, 33-35].

7. ELECTROMAGNETIC FIELDS OF SLOW BEAMS

The well-known coaxial-wire method permits the simulation of the electromagnetic field of beams with β close to unity. One may slow down the phase velocity of the simulator line by dielectric loading, but in this case the ratio of E and H does not correspond in general to that of the slow beam. In this section, small loop and probe antennas developed for transverse pick-up response measurements will be discussed.

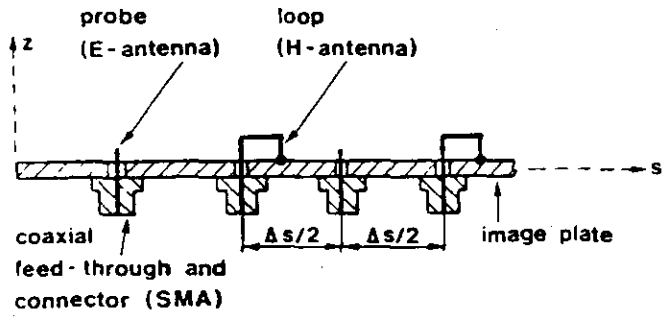

Fig. 13 - Cross section of the beam simulator for slow beams [36].

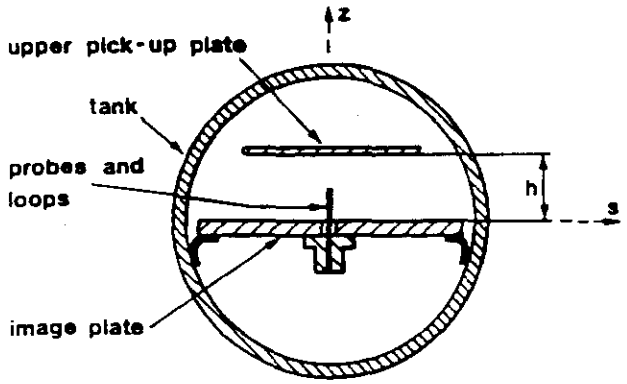

Fig. 14 - Beam simulator installed in pick-up tank [36].

The loops and probes are lined up on a metal plate with a close spacing between adjacent elements (Fig. 13). The installation in the PU tank is sketched in Fig. 14. The elements are fed via delay lines of properly adjusted length $\ell \alpha s/\beta$ to create the $e^{i\omega(t - s/\beta c)}$ dependence. The loop and

probe power levels are separately adjusted while attenuators at the entrance to the elements avoid reflections. The signal is coupled out at the normal exit port of the pick-up and displayed using the network analyzer. A simple loop-coupler type of pick-up with known response is installed downstream in the same tank for calibration.

A detailed mathematical discussion of the electromagnetic fields in this system as compared to the fields of a beam is given in Ref. [36]. It can be shown that for very slow beams ($\beta < 10\%$) most of the field energy is due to the electric field and thus only probes (E-field) are required. The other condition to be met is a sufficient line density (spatial density) of the probes and loops, which is also a function of the distance h. Their spacing Δs should not exceed $\lambda_0/2\beta$ of the highest spectral component (λ_0 = free-space wavelength).

A beam simulator with probe antennas spaced by Δs = 17 mm was used to measure the sensitivity of a pick-up for stochastic cooling at β = 0.065 (2 MeV kinetic energy) in LEAR. The device [37] tested is a slow-wave structure formed by a meander-shaped stripline coated on dielectric plates placed 30 mm above and below the beam. The phase velocity in the beam direction is matched to 0.065. In the measurement, the required electrical delay length from one probe to the next, $\Delta\ell = \Delta s/\beta$, is therefore about 260 mm.

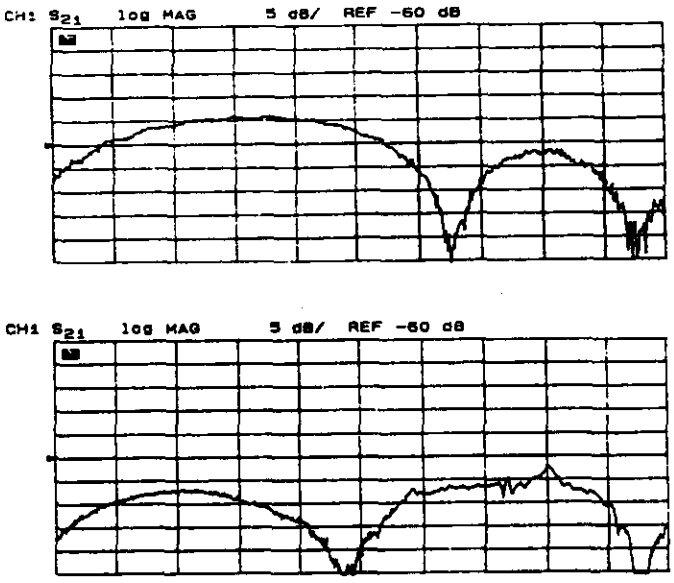

Fig. 15 - Sensitivity of meander coupler (upper curve) and loop coupler vs. frequency. Vertical scale: 5dB/div [36].

In Fig. 15 the response of the 600-mm-long meander coupler is compared to that of a 200-mm-long, solid electrode installed as a loop coupler at the same distance above the beam but downstream in the PU tank. One concludes that the longer meander structure has a 13-dB (factor 20) higher average sensitivity. At equal length, i.e. assuming several short loop couplers in series with a proper delay, this reduces to 4 dB (factor 2.5). One also notes the expected $\sin^2[\omega(\ell/2c)(\beta^{-1}-1)]$ response of the loop with the first maximum at f ≈ 50 MHz compared to f ≈ 80 MHz for the longer meander structure.

It should be stressed that with the set-up depicted in Fig. 14 nearly any ratio of E/H and any β value (including $\beta > 1$) may be adjusted independently. The probes and loops do not form a transmission line that could transport electromagnetic energy below waveguide cut-off. Thus no signal degradation, as with the conventional stripline/image plane approach, appears.

8. MEASUREMENT ABOVE THE CUT-OFF FREQUENCY

In a beam pipe with a coaxial wire the geometric dimensions define the cut-off frequency of TE and TM modes. For the empty beam pipe (without wire) these cut-off frequencies are slightly different.

The cut-off wavelength of the first waveguide mode (TE_{11} type) on a circular coaxial line is roughly equal to the mean circumference i.e. $\lambda_{c(TE_{11})} \approx \pi(r_1+r_2)$. When increasing the frequency of the network analyzer (Fig. 16) beyond this cut-off, one will already note a number of deep notches in the transmission response (S_{21}) of the reference measurement of the beam pipe. These notches are due to multipath interference effects from one or more waveguide modes with the TEM field. It is obvious that under such circumstances a "response" calibration (as the easiest calibration routine) may become meaningless. More sophisticated calibration procedures, as used for de-embedding, are by definition restricted to a single-mode case (TEM on a coaxial line and normally the fundamental mode for waveguides). The reason why these modes show such bothersome effects is that they are inevitably excited at any discontinuity, such as kinks of a taper or support disks of the center conductor. One possible way to fight the problem is by

very careful mechanical construction, e.g. smooth tapers with all edges rounded off. A serious difficulty is to position the center conductor without causing mode conversion. A very thin wire center conductor may be kept under strong mechanical tension in a special fixture at the end of the tapers [38]. Another possibility for supporting the wire with a minimum of dielectric material is by using two pairs of very thin nylon strings. But this method requires holes to be drilled into the vacuum chamber. In a recent paper [39] Lambertson et al. have proposed to introduce lossy material (absorber pads) at the ends of the tapers in order to suppress in particular the TM modes (Fig. 16). This rather easy manipulation can suppress the notches very efficiently. However, the TEM field also experiences a certain amount of additional attenuation which is, however, within an

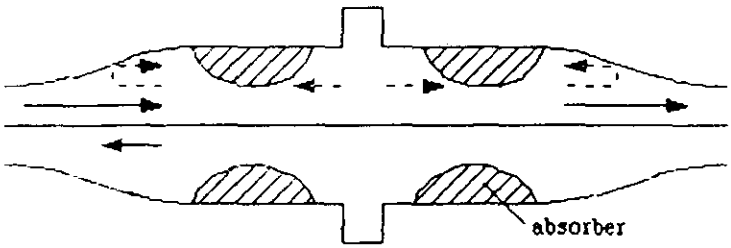

Fig. 16a - Wire with pads to absorb TM modes, shown dashed. TEM signals are shown in solid [39].

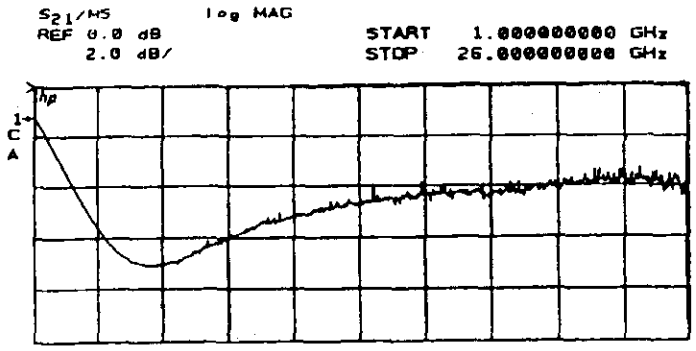

Fig. 16b - Attenuation of wire current by absorbers [39].

acceptable range (Fig. 16b) and can easily be removed by "response" calibration which is now possible. The absorber pads may be made from anechoic-chamber cladding material. Their size and position have to be determined experimentally for a given beam pipe.

For some applications it is very desirable to have a remote probe in the beam pipe without the need to pull a wire through [40,41]. In this case, the choice of selectively exciting (by means of a specially designed mode launcher) TM or TE modes exists. Since the TM_{01} waves exhibit a surface current distribution with longitudinal current only, they are better related to the TEM field than TE modes. By relating the surface current and the power flux in such TM waves, a waveguide mode impedance (frequency dependent) can be defined. It is used in the same way as Z_0 (= characteristic coaxial line impedance) to evaluate the unknown longitudinal beam-coupling impedance (transmission measurement).

If one wants just to localize a small discontinuity in a beam pipe this method may be applied similarly to the well known TDR (Time-Domain Reflectometry) on coaxial lines or optical fibers. Such measurements may be useful for acceptance tests of beam pipes of several meters length, or pipes already installed in a machine. The beam pipe is measured in analogy to a waveguide including S_{11} calibration to remove the effect of imperfections of the coaxial waveguide (= beam pipe) adapter (valid only for one mode). Depending on the cross section of the beam pipe, one often has to use TE modes for practical convenience in this band-limited waveguide TDR measurement with synthetic pulses (bandpass mode). Thus there is no direct relation to the beam-coupling impedance, but the method shows with great sensitivity the location and the approximate size (in terms of reflection coefficient) of discontinuities [42,43]. As a closing remark it should be added that during the construction of the CERN-ISR similar acceptance tests on sections of the beam pipe were carried out. However, at that time sophisticated instrumentation for synthetic pulses and waveguide S_{11} calibration was not available [44]. The beam pipe was converted into a wave-guide resonator by means of shorts at either end. Then with suitable couplers the frequencies and Q-values of the resonances were measured and compared to a reference. Significant deviations from this reference indicated that there was something different in the device tested, but normally this did not indicate the location of the fault.

9. PERTURBATION MEASUREMENTS ON CAVITIES

For experimental determination of the field distribution in a resonant cavity one usually uses a perturbation method: a small perturbing object is moved along some path through the cavity, and the resonance frequency is measured as a function of the position of this object. Perturbing objects may be dielectric or metallic bodies of revolution depending on the type of field to be measured [45]. The resonance frequency can be obtained by transforming the cavity into an oscillator by means of an external amplifier or by measuring the phase of a transmitted signal at the unperturbed frequency f_0. Q measurements are performed by taking two or more points of the resonance curve and applying an appropriate formula [46].

The frequency shift of the cavity resonance is given by

$$\frac{\omega - \omega_0}{\omega_0} = \frac{1}{W} (-K_1\varepsilon_0\hat{E}_\parallel^2 - K_2\varepsilon_0\hat{E}_\perp^2 + K_3\mu_0\hat{H}_\parallel^2 + K_4\mu_0\hat{H}_\perp^2) \tag{9.1}$$

where W is the energy stored in the cavity; $E_\parallel$, $E_\perp$, $H_\parallel$, $H_\perp$ are the electric and magnetic fields parallel and transverse to the perturbing object. The coefficients K_1 to K_4 are proportional to the electric and magnetic polarizability of the perturbing object. If the latter is elongated, K_1 is much larger than K_2, K_3, K_4: the frequency shift is then due essentially to the component of E which is parallel to the long axis of the perturbing object. If $P_\parallel$ is the electric dipole moment induced by an external electric field $E_\parallel$ in a perturbing object of length 2ℓ, we may write

$$P_\parallel = \varepsilon_0 E_\parallel \frac{4\pi}{3} \ell^3 G$$

where G is a dimensionless geometrical factor. The ratio $P_\parallel/(\varepsilon_0 E_\parallel)$ is the electric polarizability of the object. For a prolate ellipsoid [47] with semi-axes ℓ and a

$$G_{ell} = [1 - (a^2/\ell^2)]^{3/2}[\text{arc th}\sqrt{(1-a^2/\ell^2)} - \sqrt{(1-a^2/\ell^2)}]^{-1}. \tag{9.3}$$

When $\ell/a \to \infty$,

$$G_{ell} \approx [\log(2\ell/a) - 1]^{-1}. \tag{9.4}$$

The coefficient K_1 in Eq. (9.1) is directly related to the electric polarizability of the perturbing object by [45]

$$K_1 = \frac{1}{4}\frac{P_{\parallel}}{\varepsilon_0 E_{\parallel}} = \frac{\pi}{3}\ell^3 G \ . \qquad (9.5)$$

In practice the elongated object is often a cylindrical needle. Hahn and Halama [45] made a proposal to calculate K_1 of a cylindrical needle by applying a correction factor 3/2 to the electric ease of polarizability of the inscribed ellipsoid. But this correction factor depends on the shape of the needle; its correct value can be determined only by computing exactly the ease of polarizability of a needle considered as a hollow metallic cylinder [48].

The frequency shift can be measured either directly, by measuring ω at each position of the perturbing object by a fast tuning technique, or indirectly, by measuring the phase Φ of a transmitted signal at ω_0. If Φ is set to zero at the unperturbed frequency, the perturbed frequency is derived from

$$\frac{\omega - \omega_0}{\omega_0} = \frac{1}{2Q_\ell}\,\mathrm{tg}\Phi \ . \qquad (9.6)$$

When Φ is not small, because of the non-linearity of $\mathrm{tg}\Phi$, considerable errors may result on R/Q if the frequency of the transmitted signal is not exactly ω_0; this means that the unperturbed resonance frequency ω_0 must be accurately determined when the phase method is used. The same reasoning applies for Q measurements, since they are usually based on Eq. (9.6).

In practical measurements the loaded Q of the cavity should be close to the unloaded Q (= Q_0), which implies weak coupling of the input and output coupler. Single-cell and multiple-cell cavities are measured essentially in the same way, i.e. in transmission on the resonance to be considered.

For excitation of TM modes with cylindrical symmetry, on-axis probes are used, adjusted at resonance to a dip of 0.1 to 0.3 dB in reflection coefficient. In order to distinguish dipole and quadrupole modes, probe pairs and quartets may be taken for excitation and pick-up, together with broadband 3-dB, 180° hybrids. In the case of degeneracy (two modes having the same frequency), the suppression of unwanted mode may exceed 60 dB.

To measure zeropole (= cylinder symmetric) modes the perturbing object is moved along the axis of the cavity, and off-axis for dipole and higher-

order modes. The sign of the electric field may be determined by comparing the phase signals measured with a probe or loop at a set of holes drilled in the different cells (multi-cell cavity).

If it is not allowed to drill such holes into the cavity wall, usually the correct sign has to be guessed by the operator after examination of the trace that was recorded. Obviously, this is a weak point in the whole procedure and sometimes ambiguities occur. For dipole and higher-order modes, the plane of polarization must also be determined since, in general, it is not horizontal or vertical due to asymmetries on the cavity (coupling ports, etc.). An extensive description of measurements carried out on single- and multiple-cell cavities (including a discussion of many practical aspects) has been given by J. Jacob [49].

Nowadays, these measurements are usually carried out with a vectornetwork analyzer and a synthetisizer generator using the phase method. When determining the R/Q knowledge of Q is not required. The R/Q value is obtained as the result of a Fourier transform on the measured phase values as a function of the position [48-50].

With the availability of high-performance computer codes to work out electromagnetic fields in accelerator structures, often only the measurement of Q is required and R/Q is obtained from numerical calculations. But these types of perturbation methods are still needed to carry out final tuning of multiple-cell structures or RFQ's for example. The purpose of the tuning is to obtain a prescribed field pattern or a certain degree of field homogeneity in a given structure. This includes also the adjustment of the resonance frequency and coupling of each individual cell. Such measurements on multiple cells are often done in reflection and travelling-wave mode, i.e. with a terminating load at the end of the structure [51]. For adjustments of an RFQ a very special perturbing object has been used, namely a ping-pong ball [52]. This ping-pong ball could be slid along the vanes, its exact position being very critical for this type of measurement.

10. CONCLUSION

The coaxial wire method is a useful and efficient tool for (simulated) beam-coupling impedance and loss-factor measurements. Usually one obtains

reliable results for a single, localized impedance with $Z \ll Z_L$. This does not mean that in other cases (several discontinuities $Z \geq Z_L$) the results are incorrect, but caution and cross checking are required. It should be kept in mind that the wire permits coupling (= energy exchange) between two or more discontinuities, which would not be coupled in the case of an empty beam pipe. In general, transmission rather than reflection measurements are better. The effect of multiple reflections due to mismatch in adapter pieces can be eliminated by time filtering (= gating).

As a second choice de-embedding (calibration) procedures may be used, as they are more difficult to handle than gating, but sometimes also more effective in rejecting undesired signals. In all cases a high electrical and mechanical repeatability is required.

The beam-coupling impedance and the loss factor can be measured with the same instrumentation using the synthetic-pulse technique. Synthetic pulses are more powerful in terms of stability and signal-to-noise ratio than real pulses but the set-up may be more expensive. Caution should be exercised for frequencies beyond waveguide cut-off, and the effect of waveguide modes must be carefully considered. Impedance measurements without a coaxial wire relying on TM modes appear to be possible within certain limitations. Band-limited Time Domain Reflectometry (TDR) using TM or TE modes can return useful information on beam pipe discontinuities. In order to simulate transverse fields of very slow beams, an array of probe and loop antennas gave promising results.

Bead-pull measurements on cavity-like objects are nowadays used rather for tuning purposes (multiple cell, RFQ) than for R/Q determination. With the availability of powerful computer codes for field calculation, often only the Q measurement is still required.

ACKNOWLEDGEMENTS

The author would like to thank G. Dôme, G. Jackson, D. Möhl, C. Taylor and B. Zotter for many helpful and enlighting discussions and contributions, as well as A. Molat-Berbiers for typing the manuscript.

REFERENCES

[1] J.D. Jackson, Classical Electrodynamics, John Wiley and Sons, New York 1975, Sect. 9.1.

[2] E. Karantzoulis, An Overview on Impedance Measuring Methods for Accelerators, Sincrotrone Trieste, ST/M-91/1, January 1991.

[3] S.A. Heifets and S.A. Kheifets, Coupling Impedance in Modern Accelerators, SLAC-PUB-5297, Sept. 1990.

[4] L. Palumbo and V.G. Vaccaro, Wake Fields Measurements, Joint US-CERN School on Particle Accelerators, Lecture Notes in Physics, No. 343, Springer-Verlag, 1988.

[5] R.L. Gluckstern and R. Li, Analysis of Coaxial Wire Measurement of Longitudinal Coupling Impedance, 4th Int. Conf. On High-Energy Accelerators, KEK, Japan, 1990.

[6] T. Weiland, On The Numerical Solution of Maxwell's Equations and Applications in the Field of Accelerator Physics, DESY M-84-06, Jan. 1984.

[7] M. Sands, J. Rees, SLAC-report PEP-95, August 1974.

[8] P.B. Wilson, J.B. Styles and K.L.F. Bane, Comparison of Measured and Computed Loss to Parasitic Modes in Cylindrical Cavities with Beam Ports, SLAC-PUB-1908, PEP-240, March 1977.

[9] H. Hahn and F. Pedersen, On Coaxial Wire Measurements of the Longitudinal Coupling Impedance, BNL 50870, Particle Accelerators and High-Voltage Machines - TID-4500, April 1978.

[10] M. Billing (Cornell), Private Communication.

[11] F. Caspers, Beam Impedance Measurement Using the Coaxial Wire Method, Proc of the Workshop on Impedance and Current Limitations, ESRF Grenoble 1988, Sect. 2.1, and CERN PS/88-59 (AR).

[12] K. Lange, K.H. Löcherer, Taschenbuch der Hochfrequenztechnik (4 Auflage, 1986), Springer Verlag, p. C20, 1986.

[13] D. Boussard, H. Henke, J. Gareyte, Academic Training Programme, CERN, 1986, Unpublished.

[14] F. Caspers, Beam Impedance Measurement by the Wire Method Using a Synthetic Pulse Technique, IEEE, NS-32, pp. 1914-1916, 1985.

[15] M.E. Hines, H.E. Stinehelfer, Time-Domain Oscillographic Microwave Network Analysis Using Frequency-Domain Data, IEEE Trans. on Microwave Theory and Techniques, Vol. MTT-22, No. 3, March 1974.

[16] J. Curran, Applying TRL Calibration for Non-Coaxial Measurements, Microwave System News, pp. 91-98, March 1988.

[17] L. Walling, LANL, Private Communication.

[18] L. Walling, D. McMurray, D. Neuffer, H.A. Thiessen, Transmission Line Impedance Measurements for an Advanced Hadron Facility, LANL 1988.

[19] H.J. Eul and B. Schiek, Experimental Results of New Self-Calibration Procedures for Network Analyzers, Proc. of the 20th European Microwave Conf., Budapest, 1990, 1461-1466.

[20] H.J. Eul and B. Schiek, Broadband Self-Calibration Techniques for Network Analyzers, Frequenz 44 (1990), 5.

[21] H.J. Eul, Comments on "A Unified Mathematical Approach to Two-Port Calibration Techniques and Some Applications", IEEE Trans. on Microwave Theory and Techniques, Vol. 38, No. 8, August 1990.

[22] G.F. Engen and C.A. Hoer, "Thru-Reflect-Line": An Improved Technique for Calibrating the Dual Six-Port Automatic Network Analyzer, IEEE Trans. on Microwave Theory and Techniques, Vol. MTT-27, No. 12, Dec. 1979.

[23] R.R. Pantoja, M.J. Howes, J.R. Richardson and R.D. Pollard, Improved Calibration and Measurement of the Scattering Parameters of Microwave Integrated Circuits, IEEE Trans. on Microwave Theory and Techniques, Vol. 37, No.11, Nov. 1989.

[24] R.A. Soares, P. Gouzien, P. Legaud and G. Follot, A Unified Mathematical Approach to Two-Port Calibration Techniques and Some Applications, IEEE Trans. on Microwave Theory and Techniques, Vol. 37, No. 11, Nov. 1989.

[25] R.A. Speciale, A Generalization of the TSD Network-Analyzer Calibration Procedure, Covering n-Port Scattering-Parameter Measurements, Affected by Leakage Errors, IEEE Trans. on Microwave Theory and Techniques, Vol. MTT-25, No. 12, Dec. 1977.

[26] H.J. Eul and B. Schiek, Thru-Match-Reflect: One Result of a Rigorous Theory for De-embedding and Network Analyzer Calibration, Proc. of the 18th European Microwave Conf., Stockholm, 1988.

[27] King-Yuen Ng, Impedances of Stripline Beam-Position Monitors, Particle Accelerators, 1988, Vol. 23, 93-102.

[28] G. Nassibian, The Real Part of the Low Frequency Beam Impedance of Travelling Wave Kickers with Arbitrary Terminations, CERN/PS/85-68 (BR), 1985.

[29] G. Nassibian and F. Sacherer, A Method for Measuring Transverse Coupling Impedance, CERN/ISR-TH/77-61, 1977.

[30] G. Lambertson, Dynamic Devices-Pickups and Kickers, FNAL Acc. School 1984, AIP Conf. Proc. 153, 1413-1442.

[31] H. Henke, Private Communication.

[32] S. Kheifets and B. Zotter, Longitudinal and Transverse Impedance of Bellows in the Low Frequency Range, Nucl. Instr. and Methods in Physics Res., A243, 13-27, 1986.

[33] F. Caspers, J.P. Delahaye, J.C. Godot, K. Hübner and A. Poncet, EPAC, Rome, 1988, CERN PS/88-37 (LP).

[34] A. Faltens, E.C. Hartwig, D. Möhl, and A.M. Sessler, An Analog Method for Measuring the Longitudinal Coupling Impedance of a Relativistic Particle Beam with its Environment, Proc. 8th International Conf. on High Energy Acc. CERN 1971.

[35] L.J. Laslett, K. Neil, A. Sessler, Transverse Resistive Instabilities Rev. Sci. Instr. 36, pp. 436-448, 1965.

[36] F. Caspers, D. Möhl, and A. Schwinn, A New Bench Method to Simulate Electromagnetic Fields of Slow Beams, EPAC 90 and CERN/PS 90-35 (AR).

[37] N. Tokuda, Travelling Wave Pick-ups and Kickers for Stochastic Cooling at Low Beam Velocity, in: Proc. IVth LEAR Workshop, Villars (CH), 1987, (Edited by C. Amsler et al.) Harwood Academic Publishers, Chur 1988, pp. 135-138.

[38] G. Jackson, FNAL, Review of Impedance Measurements at FNAL, 1990, unpublished.

[39] G.R. Lambertson, A.F. Jacob, R.A. Rimmer, F. Völker, Techniques for Beam Impedance Measurements Above Cut-off, LBL-28190, EPAC Rome 1990.

[40] R.A. Rimmer, D.A. Goldberg, A.F. Jacob, G.R. Lambertson, F. Völker, Beam Impedance Measurements on the ALS Curved Sector Tank, LBL-28192, EPAC Rome 1990.

[41] A. Jacob and G.R. Lambertson, Impedance Measurements on Button Electrodes, IEEE Part. Accel. Conf., Chicago 1989, LBL-25955.

[42] P.I. Somlo, The Locating Reflectometer, IEEE Trans. on Microwave and Techniques, Vol. MTT-20, No. 2, Feb. 1972.

[43] D. Stone, K.L. Felch and S.T. Spang, Mode-Specific Reflectometry in a Multimode Waveguide, IEEE Trans. on Microwave Theory and Techniques, Vol. MTT-31, No. 9, Sept. 1983.
[44] C. Taylor, Private Communication.
[45] H. Hahn and H.J. Halama, Perturbation Measurement of Transverse R/Q in Iris-Loaded Waveguides, IEEE Trans. on Microwave Theory and Techniques, MTT-16, Jan. 1988, 20-29.
[46] L.G. Bernier, T. Sphicopoulos and F.H. Gardiol, An Automatic System for the Measurement of the Field Distribution in Resonant Cavities, IEEE Instrum. and Methods, IM-32, Dec. 1983, 462-466.
[47] L.C. Maier and J.C. Slater, Field Strength Measurements in Resonant Cavities, J. Appl. Physics, Vol. 23, No. 1, Jan. 1962.
[48] F. Caspers and G. Dôme, Precise Perturbation Measurements of Resonant Cavities and Higher Order Mode Identification, CERN SPS/85-46 (ARF), 1985.
[49] J. Jacob, Measurement of the Higher-Order Mode Impedances of the LEP Cavities, ESRF-MAC-06/10, 1988.
[50] P. Marchand and D. Proch, Higher Order Mode Measurements in a 5-Cell Copper Cavity at 2 GHz and Application to a Superconducting Cavity for Petra, CERN/EF/RF 82-7, Oct. 1982.
[51] Lapostolle and Septiev, Linear Accelerators, 1970 North-Holland Publishing, 91-100.
[52] W. Pirkl, Tuning of the RFQ, CERN-PS/RF Note 83-4, 1983.